Anal Bioanal Chem (2006) 385: 568–585
DOI 10.1007/s00216-006-0412-7

REVIEW

Arne Bengtson · Thomas Nelis

The concept of constant emission yield in GDOES

Received: 22 December 2005 / Revised: 27 February 2006 / Accepted: 2 March 2006 / Published online: 4 April 2006

Abstract This review paper describes the evolution of the quantification procedure for compositional depth profiling (CDP) in glow discharge optical emission spectrometry (GD-OES), based on the constant emission yield concept. The concept of emission yield (EY) is defined and ways of measuring it experimentally are discussed. The history of the development of quantitative CDP is reviewed, which shows that all of the different approaches depend on the assumption that the EY is essentially a matrix-independent quantity. Particular emphasis is placed on the dependence of the EY on the plasma parameters of current, voltage, power and pressure. In short, impedance changes (current voltage) can significantly affect the emission yield and should either be corrected mathematically or the impedance should be kept constant by pressure regulation in order to obtain reliable results from GDOES CDP. On the other hand, the effect of varying the pressure on the emission yield can be considered to be minor within the limits of practical operating conditions for most CDP applications. It is worth, however, bearing in mind that varying the discharge pressure has a significant effect on the plasma processes, and does affect the emission yield when these variations are large. The experimental results obtained for the emission yield are related to the results from theoretical model calculations published on the subject.

A. Bengtson
KIMAB,
Drottning Kristinas väg 48,
11428 Stockholm, Sweden

T. Nelis
Swiss Federal Laboratories
for Materials Testing and Research (EMPA),
Feuerwerkerstrasse 39,
3602 Thun, Switzerland

T. Nelis (✉)
Atout and Progrès,
10 rue de la paix,
75002 Paris, France
e-mail: ThoNelis@aol.com
Tel.: +33-62-4454383

Keywords Glow discharge optical emission spectroscopy · Emission yield · Compositional depth profiling

Introduction

Glow discharges (GD) have been studied for many years now [1]. In fact, glow discharges have been used for analytical purposes for about 100 years [2]. Today we know of many different glow discharges [3–5] and even in the analytical field the variety of glow discharges used is very wide [6]. In this review, however, we will concentrate on the properties of the "hollow anode–flat cathode" glow discharge introduced by Grimm [7] in 1967 and now commonly called "the Grimm source." In the following we use the term glow discharge to mean a "Grimm-type" glow discharge operating at typical conditions of 5–10 hPa pressure and usually at powers of less than 100 W.

One of the most important properties of a glow discharge, from an analytical viewpoint, is the separation of sputtering and excitation. Analyte material is first sputtered from the sample surface; it then moves through the cathode dark space into the negative glow region, where it gets excited and/or ionized through collisions with other species present in the plasma. While the sputtering process is by its nature very much dependent on the properties of the analyte sample and its surface, the excitation process is thought to be dependent in only a minor way on the material analyzed. The idea that the light emission process is independent of the sample analyzed is critical to the easy quantification of compositional depth profiling (CDP). The question of how close this assumption is to reality is one of the major subjects of this review article.

Operational principles of the technique

Basic plasma processes in the Grimm-type glow discharge

The Grimm-type GD source consists of an anode tube and the sample to be analyzed. The flat sample is placed

perpendicular to the front of this anode tube. The anode tube is usually kept at ground potential. Electrical power, either dc or rf, is supplied directly to the sample. A spacer maintains the sample surface at a distance of between 0.1 and 0.2 mm from the anode tube. The distance between the sample and the anode is less than the thickness of the cathode dark space (CDS) in order to limit the cathode area. Sufficient vacuum tightness is achieved by an O-ring separating the discharge chamber from the air environment.

When the plasma is ignited inside the plasma chamber, free electrons and a plasma formed from gas ions are generated. Both species will move freely in the electrical field reigning in the plasma chamber and will influence this field through the creation of local charge distributions. Different characteristic areas are established in the glow discharge plasma. Two of them are crucial to the use of the GD for analytical purposes: the negative glow (NG), free of electrical field but showing high charge density for both ions and electrons, and the cathode dark space (CDS). The latter is characterized by a strong electrical field that attracts the positive ions towards the cathode, generating material erosion or sputtering. This ion bombardment also sets free secondary electrons which are then accelerated in the electrical field towards the negative glow, where they lose their energy through collisions. During these collisions they participate in excitation and ionization processes and thus maintain the plasma [3].

The sputtering process depends strongly on the sample material and its surface properties, but once the atoms are sputtered, they move as single atoms into the negative glow where they are diluted in the argon carrier gas. The sputtering process is not element-specific. All elements at the sample surface are sputtered at the same rate, at least once the equilibrium situation is found. Preferential sputtering of some elements does not play a significant role in GD-OES, because the sputtering ions bombarding the surface have a rather low energy of 100 eV. The knock-on effect, leading to significant atomic mixing in the layer structure near the surface, is very weak in GD-OES [8]. The excitation and ionization processes take mainly place in the negative glow. Its properties, and consequently the ionization or excitation yields, are independent of the properties of the sample surface, at least to a first approximation. The excitation and ionization processes are, however, strongly element-specific. For emission processes they are even specific to each spectral line. Due to the fact that matrix effects are relatively minor, the quantification of GDOES signals is relatively straightforward, at least in comparison with other depth profiling techniques such as AES, XPS and SIMS. For bulk analysis, comparisons are often made with spark OES, which is the by far most commonly used source for this purpose. Proponents of GDOES have sometimes made exaggerated claims concerning the advantages over spark; for example, that the narrower emission lines drastically reduce the extent of line interference from other elements in GDOES. While it is true that the intrinsic line widths of 0.1–0.5 pm is about ten times less than in a spark source; this is of no practical consequence since the approximately 10 pm resolution of the best analytical spectrometers is significantly wider than the line widths of both sources. Furthermore, it is often stated that glow discharge can more easily accommodate several alloy types in one calibration than spark, but in practice the difference is minor and of little analytical importance as long as the base (matrix element) is the same. The small differences are normally well-handled by the so-called multiplicative corrections routinely used in spark OES. One notable difference between the two sources is that spark calibration curves are, generally speaking, more nonlinear than those from a glow discharge, due to a higher degree of self-absorption. Again, this is of very minor practical analytical importance since second- or third-order calibration curves easily handle this type of nonlinearity. The crucial difference between the sources is that the highly "diluted" glow discharge plasma results in the matrix-independent emission yields that are the focus of this article. Therefore, GDOES permits truly multimatrix calibration, something that is not possible with a spark source.

The different processes in the negative glow leading to the observed light emission are rather complex. A list of the most important processes is given in Table 1 [9]. Which process dominates depends strongly on the reaction rate constants or the collision cross-section.

Principal excitation processes in the glow discharge

The model calculations that have been published have mostly used copper as the test cathode material. Much information on processes relating to Cu is therefore available. It is more difficult to obtain detailed information on other atoms. It is, however, unlikely that atoms like iron and manganese behave very differently, except for special cases of resonance effects, such as seen for Cu II 224 nm

In 1998, Bogaerts and Gijbels [64, 10] listed the different excitation and loss processes and their relative importance when populating and depopulating the excited states of copper. The atomic states are predominantly populated by electron impact excitation. The excited states are depopulated by radiative decay and further electron impact reactions. Copper ions in lower excited states are created by Penning ionization. The generation of the $^3P_2$ state is strongly enhanced by symmetric charge transfer reactions. The higher excited states are populated by electron impacts on copper ions in lower-lying electronic states. Atomic and ionic states therefore clearly have different excitation

Table 1 Most important excitation mechanisms in the Grimm-type glow discharge [64]

Electron impact excitation and de-excitation between levels from ground state
Excitation and de-excitation, due to collisions with argon gas
Electron impact ionization form the ground state
Penning ionization, due to collisions with metastable Ar atoms
Three-body recombination where the third body is an electron
Asymmetric charge transfer, due to collisions with Ar ions

mechanisms. It should not be surprising if their emission yields show a different dependence on the excitation parameters.

The emission yield, or the probability of emitting a photon per sputtered atom, depends on the rate constants of the above-mentioned processes. Population and depopulation of excited states also strongly depends on the spatial overlap of the copper atom population with the free electron population, as described in Eq. 1.

$$\frac{dn_{A^*}}{dt} = \int_V \int_E r(E) \cdot n_{e^-}(E, \overrightarrow{r}) \cdot n_A(\overrightarrow{r}) \cdot dE \cdot dV \qquad (1)$$

where n_{A*}, n_A, n_{e^-} are the number densities of the excited atoms, ground state atoms and electrons respectively; $r(E)$ is the excitation rate constant; V is the discharge volume and E is the electron (impact) energy.

One extreme example illustrating the importance of the overlap of the two population densities is the CDS. The copper atom density is high, but the electron density is very low. As a result hardly any light is generated in the cathode dark space. The name is obviously well chosen.

In the following we will describe the different plasma parameters and their links to the properties of the plasma. Given the complexity of plasma processes, this description can be only approximate, but it should aid the understanding of emission yields and their dependence on plasma parameters.

Descriptions of the different physical parameters and their links to fundamental properties of the plasma

The *particle density*, together with the atom radius, determines the mean free path (Eq. 2) in the hardcore model. The mean free path is a crucial parameter when describing the processes leading to light emission.

$$l = \frac{1}{\sqrt{2}\pi d^2 n^*} \qquad (2)$$

where l is the mean free path, d is the diameter of the atom and n^* is the particle density.

The atom radius of Ar is 8.8×10^{-11} m. Assuming a gas temperature of 600 K and a pressure of 800 Pa, the mean free path for argon is 75 μm.

The gas *pressure* and temperature together define the particle density in the glow discharge volume. For argon, a monoatomic inert gas, the ideal gas laws can be assumed to hold in the pressure and temperature range under study.

The gas *temperature* in a Grimm-type glow discharge is not known with precision. Temperature values frequently assumed range from 500 K to 1,100 K depending on the operating conditions and the authors [11]. It is generally assumed that the gas temperature increases with the discharge current. In some model calculations, the gas temperature is adapted to reproduce experimentally observed current–voltage characteristics. The lack of information on the temperature in the glow discharge is obviously a serious handicap when modeling analytical GDs and interpretating results from the model.

The *discharge current* is generated by the flow of positively charged ions (Ar^+) and electrons. Since both particles move in opposite directions, the two current components add together to form the discharge current (Eq. 3). Depending on the plasma area, the relative importance of the two components changes. Due to high electron mobility, the electron current is dominant in most parts of the plasma, except in the CDS. The current in the CDS is dominated by ion movement. The secondary electron emission yield describes the number of electrons removed from the cathode surface per incoming ion. For conducting material, γ ranges from 0.05 to 0.16. The ion current therefore represents 85–95% of the total discharge current in the CDS (Eq. 3).

$$i_g = i_{Ar^+} + i_{e^-} = (1+\gamma) \cdot i_{Ar^+} \qquad (3)$$

where i_g is the discharge current and i_{Ar^+} and i_{e^-} are the two components due to the movements of Ar ions and electrons, respectively.

A discussion of the discharge current is more complex in the case of rf discharges [12]. The time-averaged current is necessarily zero, due to the capacitive coupling. The current in the CDS is dominated by the ions during most of the rf cycle, except during the short moment when the sample attracts the electrons, to compensate for the ion current.

The *ion current* flowing between the plasma and the cathode is determined by the plasma ion density, the electrical field that accelerates the ions towards the cathode, and the ion mobility.

$$i_{Ar^+} = S \cdot q \cdot \langle \nu \rangle \cdot n_{Ar^+} \qquad (4)$$

where S is the CDS cross-section, q is the ion charge, $<\nu>$ is the average ion speed, and n_{Ar+} is the ion density.

The discharge current is therefore an approximate measure of the ion density in the plasma, but the ion mobility also influences the discharge current. The ion mobility depends on the gas pressure and temperature. It is obviously linked to the mean free path of the ions in the surrounding argon. Since the mean free path is of the same order of magnitude as the cathode dark space, it is difficult to derive a simple model for estimating the drift speed. For "normal" plasma conditions, an Ar^+ ion will suffer about ten collisions on its way from the NG to the cathode. We can neither assume free ion movement nor can we assume that the number of collisions between ions and Ar atoms on the way to the cathode is large, but we can reasonably assume that the drift velocity is reduced as the particle density is increased, either through a decrease of temperature or an increase in pressure. The situation is in fact even more complex, because the ions are accelerated towards the cathode and the mean drift speed $<\nu>$ consequently increases towards the cathode [13]. The CDS does not resemble an ion drift cell. The ion mobility varies with the

electrical field. The electrical field is determined by the voltage drop between the negative glow and the cathode, and the thickness of the cathode dark space.

The *voltage* usually measured is the potential difference between anode and cathode; this is usually known as the discharge voltage. In a Grimm-type source this voltage is very close to the potential difference between the negative glow and the cathode, since the potential difference between the anode and the negative glow is relatively small. The largest voltage drop is observed in the cathode dark space. The discharge voltage is therefore a measure of the total energy a charged particle (ion or free electron) can acquire during its acceleration in the CDS. When colliding with other species in the CDS, the charged particles may transfer part of the energy gained during the acceleration process and therefore never gain the maximum energy. Nevertheless, the energy has been transferred to particles participating in plasma processes.

The discharge voltage is linked to the electrical field E and the sheath thickness d by Eq. 5.

$$V = \int_0^d E(x) \cdot dx \tag{5}$$

where V is the potential difference across the CDS, d is the thickness of the CDS and E is the x component of the electrical field vector.

The *electrical field* in the CDS is directly linked to the ion density distribution in the CDS via Eq. 6. The electron density can be generally neglected as they rapidly move out of the CDS due to their high mobility.

$$\varepsilon_0 \cdot \vec{\nabla} \cdot \vec{E} = q \cdot n_{Ar^+} \tag{6}$$

where ε_0 is the dielectric constant of vacuum, $\vec{\nabla}\vec{E}$ is the gradient of the electrical field, q is the ionic charge, and $n_{\mathrm{Ar+}}$ is the ion density.

Assuming a constant ion density in the CDS [14], the electrical field will increase linearly in the CDS, so the integral relation of Eq. 5 can be simplified to Eq. 7.

$$V = 2 \cdot d \cdot E_{\max} \tag{7}$$

where V is the potential difference across the CDS, d is the thickness of the CDS and $E_{\max}$ is the maximum value of the linearly increasing electrical field.

Experimental determination of emission yields

When discussing emission yields, it is not only important to define this quantity, but also to investigating different experimental methods of measuring it and the systematic errors associated with these measurements. The emission yield for a specific spectral line is defined as the light intensity emitted at this wavelength per sputtered atom. When emission yields are experimentally measured, they are usually determined by normalizing the measured intensity to the sputtering rate-corrected concentration, and they are expressed as intensity per sputtered mass unit. This quantity does not exactly describe the emission yield, as defined above. Apart from a scaling factor, there are various processes that can make these two quantities different to each other. For extended sources, such as the glow discharge source, the emitted light can be reabsorbed by other atoms present in the plasma. This well-known phenomenon is called self-absorption and is sometimes dealt with under the name escape factor. Another source of difference between these two quantities is the varying reflectivity of the sputtered sample surface, in particular for end-on observation.

The instrumental function is crucial when comparing the intensities of different spectral lines. It is still impossible to design an achromatic optic for use over a wide spectral range of interest, from 800 nm to 120 nm. It should be clearly stated that a higher detection level does not necessarily imply a higher emission level, at least when spectral lines of very different wavelengths are compared. However, this instrumental function will not influence the detection of variations in emission intensity from one specific spectral line with varying plasma parameters. It is therefore of little relevance to this work.

In the following we discuss the different factors that influence experimentally determined emission yields.

Self-absorption

Self-absorption is caused by an atom reabsorbing a photon emitted by another atom. In order to observe this effect it is sufficient to ensure that there are a large number of atoms at the lower energy level of the transition. Compared to other OES systems, such as spark emission, self-absorption is weak in GDOES. However, it can be observed on most resonance lines when calibration ranges are sufficiently high [15]. The importance of the self-absorption effect depends on the density of atoms at the absorbing electronic levels and the oscillator strength. Light absorption follows the exponential Lambert–Beer rule; it is therefore a nonlinear effect and tends to bend the calibration curves. Increasing the content of the element appears to reduce the spectral line sensitivity.

$$K_L \propto s_L(f_{li} \cdot c_l \cdot q_M) \tag{8}$$

$$s_L = \sqrt{\frac{\pi}{2\ln(2)R}} \cdot \frac{10^4}{(4\pi)^2} \cdot \sqrt{\frac{M}{T}} \cdot \lambda^3 \cdot \frac{g_j}{g_i} \cdot A_{ji} \tag{9}$$

where K_{L} is the optical depth, f_{il} is the fraction of the element l in the lower state i of the transition, s_{L} is the

effective absorption cross-section, M is the atomic mass, T is the gas temperature, and g_j and g_i are the multiplicities of the higher and lower states, respectively. A_{ji} is the atomic transition probability.

More detailed discussions of the effect and its application to GDOES can be found in publications by Payling [16], Bogaerts et al. [17] and Weiss [18]. When measuring emission yields for resonant lines, it is important to note that changing the sputtering rate will change the level of self-absorption, and it will therefore influence the observed signal strength. It is not only transitions to the ground-state that are affected by self-absorption; even transitions to higher excited states may exhibit self-absorption as long as these states are sufficiently well-populated (for example the metastable Cu (3d9 4s2) state [19]).

Surface reflectivity

When measuring highly polished samples with a transparent layer, a peculiar interference pattern can be observed. These oscillations in the intensity, when observed end-on, are explained by multiple reflection of the light emitted by the plasma on the sample surface and the layer–substrate interface [20]. The effect has since been well-described in the literature [21, 22] and is not the subject of this review article. However, these oscillations are a clear indication that light reflection on the sample surface is not negligible in GDOES; even if the sample is not coated with a transparent film, some part of the light will be reflected off the sample surface and detected by the spectrometer. The reflected light may in some cases represent 20% of the detected signal. In the absence of a quantifiable interference effect it will be difficult to estimate the intensity of reflected light. This effect will lead to errors when determining the emission yield. Highly polished sample surfaces will be able to reflect more of the light back to the spectrometer than rough surfaces. However, for most metallic materials the surface structure will be modified by the sputtering, as crystalline structures will appear. The intensity of the reflected light will therefore vary as the sputtering continuously modifies the sample surface.

Most real-world applications involve relatively rough sample surfaces; in this case the reflected light contributes only a few percent to the overall emission yields.

Sputtering rates

Emission yields are experimentally determined by dividing the observed line intensities by the sputtered mass. The sputtering rate, SR, must therefore be determined. Although sputtering rate measurements can be made with a relatively high precision [23] of 3%, these measurements are fairly time-consuming and can lead to a relative standard deviation of 10% when a large number of measurements need to be performed, which is the case in detailed studies of the emission yield and its variation with the parameters of the plasma.

Development steps in CDP quantification

In depth profiling, complete quantification includes both the elemental composition and the depth. This is different from bulk analysis, where only the composition needs to be quantified. In several other surface analytical techniques, the composition and depth rely on separate calibrations. Therefore, several early attempts to develop quantification methods for GD-OES also relied on separate calibrations [24]; see next section. For determinations of bulk elemental composition, it is a very common technique to make use of an "internal standard" in the form of the signal from the major (matrix) element, such as Fe in steels. However, this is not applicable in general for depth profiling, since different surface layers often have completely different compositions. These challenges made it necessary to develop novel ideas and techniques in order to be able to quantify GD-OES depth profiles, eventually leading to the introduction of the concept of the emission yield, which resolved the dilemma in an elegant way.

Early work on quantification and the emission yield concept

Experimentally, it is easy to show that the emission intensity of an analytical line in a GD is not just proportional to the concentration of the corresponding element in the sample. The observed light intensity also depends on the sputtering rate of the sample. Intuitively, this observation is easily understood. The photons are generated in the negative glow. The emission intensity should therefore be proportional to the sample atom density in the plasma, which in turn is directly linked to the sputtering rate. If we allow the discharge parameters (voltage, current, power and pressure) to vary, the situation becomes more complex. However, as long as the excitation conditions in the plasma remain at least nearly constant, the sputtering rate–intensity proportionality provides an elegant solution to the quantification problem. The basic assumption is that the integrated intensity from one element and spectral line is exclusively proportional to the sputtered mass of that element. This implies that the emission yield is independent of the sample matrix. In 1984 Takadoum et al. [25] introduced the concept of *emission yield* (EY), making use of the similarity between SIMS and GDOES in order to develop a quantification method. The EY can be expressed as the emitted light per unit sputtered mass of an element according to the following equation (Eq. 10):

$$R_{ij} = \frac{I_{ijb}}{c_{ib} q_b} \tag{10}$$

where I_{ijb} is the emission intensity of spectral line j of element i in sample segment b; c_{ib} is the concentration of element i in sample segment b; q_b is the sputtering rate in sample segment b; R_{ij} is the *emission yield* of spectral line j of element i.

The EY is an atom- and instrument-dependent quantity, which must be determined (calibrated) independently for each spectral line and instrument. In the method of Pons-Corbeau et al. [26], they set up a method where ratios of the EY of each analyte to that of the major element in the matrix were used to calculate the concentrations. The concentration c_{ib} of element i in sample segment b was then expressed as:

$$c_{ib} = \frac{I_{ib}R_{maj}/R_i}{I_{maj} + I_1R_{maj}/R_{1b} + I_2R_{maj}/R_{2b} + \ldots} = c_{ib} = \frac{I_{ib}/R_i}{\sum_i I_i/R_{ib}} \tag{11}$$

where the suffix *maj* denotes the matrix element, for example Fe. This equation (Eq. 11) is useful because it simplifies the calibration in two cases commonly encountered in applications for the steel industry [27]:

- When the matrix concentration is close to 100%, it is sufficient to determine the relative intensity of each analyte versus that of the matrix element since summing over other analytes adds little to the denominator in Eq. 11;
- For binary systems, such as ZnNi and ZnFe metallic coatings, Eq. 11 becomes very simple and the relative emission yields are easily determined.

One disadvantage of using Eq. 11, apparently overlooked by Pons-Corbeau et al., is that the information about sputtering rates, and therefore the depth information, is lost. Therefore, they could only determine elemental concentrations as a function of time, and they estimated the depth using separate measurements of the SR in each material investigated. In a recent publication by Nelis et al. [28], the idea of using relative intensities has been extended. In this work the calibration functions are deduced using relative concentrations and intensities.

$$\left(c_i/c_{maj}\right) = f\left([a_i]; I_i/I_{maj}\right) \tag{12}$$

where $[a_i]$ represents a set of regression parameters.

The concentration of the major element c_{maj} and consequently the absolute concentrations of the minor elements can be calculated by normalizing the sum of all concentrations to 100%:

$$c_{maj}^{rel} = \frac{1}{1 + \sum c_i/c_{maj}} \tag{13}$$

The sputtering rate can be calculated by comparing the concentration of the major element to the sputtering rate-corrected concentration of the major element.

$$q = c_{maj} \cdot q \Big/ c_{maj}^{rel} \tag{14}$$

In another early publication from 1984 on quantitative depth profiling from K. Suzuki et al. [29], the concept of EY was not used directly. The correlation between SR and emission intensity was understood, but this was handled by expressing the intensity for each element as a linear combination of terms from all elements according to their concentrations.

$$c_i = I_i/I_{i(100)} \times \left[1 + \sum_j \alpha_j(c_j)\right] \tag{15}$$

where $I_i/I_{i(100)}$ is the relative intensity of the metal i when compared to the pure metal; $\alpha_j(c_j)$ is the correction term for the matrix effect by element j. This term is actually a polynomial up to third order.

For a test specimen where c_i is unknown, the relative intensity $I_i/I_{i(100)}$ is initially used as an approximation, and Eq. 15 is iteratively calculated until c_i converges to a stable value.

The same type of equation was used to express the SR, determined by an iterative calculation. This method was quite adequate for binary alloy coatings , but was quickly abandoned as a general solution to the quantification problem. Just one year later, M. Suzuki et al. (with K. Suzuki as coauthor!) published a paper [30] where the EY concept was first used in the way that now has become the most common technique: determination of sputtered mass/element, derived from (Eq. 10).

$$\delta m_{i,b} = c_{i,b} \cdot q_b \cdot \delta t_b = I_{i,j}\delta t_b \big/ R_{i,j} \tag{16}$$

where $\delta m_{i,b}$ is the sputtered mass of element i in segment b during time increment t_b.

Calibration to determine the emission yields $R_{i,j}$ is performed using calibration samples, preferably CRMs. These samples are normally of bulk type with known concentrations, in which case it is necessary to determine the sputtering rate (SR) of each calibration sample. Alternatively, samples with coatings of known composition and thickness may be used, in which case the SR is given by the penetration rate of the coating. In each depth segment b, the concentration of each element c_{ib} is calculated by sum normalization to 100%.

$$c_{ib} = 100 \times \delta m_{ib} \Big/ \sum \delta m_{ib} \tag{17}$$

The total sputtered mass in each segment is given by the sum in the denominator of Eq. 17. The truly elegant aspect of this technique is that the determination of the total sputtered mass gives information on the sputtered depth. However, converting the sputtered mass to depth requires a calculated estimate of the density of the material, which introduces some uncertainty. This, however, is not the subject of the current review article. More detailed information on the subject can be found in Payling [31] and Nelis [32].

In the early papers discussed above, there is no mention of the effect of variations in the discharge parameters; these are assumed to be fixed for each selected application. In another early paper on quantification, Bengtson pointed out that, in addition to the SR, at least one of the electrical discharge parameters (voltage and current) varies as layers of different composition are penetrated in a depth profile analysis [33]. At that time (1985), all of the commercially available GD sources could only be operated with constant pressure, and due to variations in the electrical characteristics of the sample (cathode) material, such variations were inevitable in several technically important applications. As an example, a hot dipped Zn coating on steel was profiled with the source run in constant pressure–constant current mode. The voltage increased from 510 V in the Zn to 740 V in the steel, with a gradual increase in the analytically important interface region. Bengtson assumed that such variations affect the excitation probability (which in turn determines the EY) and must therefore be taken into account during quantification. Therefore, an empirical intensity expression was derived from a set of experimental data. Argon lines were studied in an attempt to separate the effects of sputtering rate variations from those of excitation probability. The resulting expression for the analyte line intensities incorporates all of these effects.

$$I_{j,b} = k_j \cdot c_{i,b} \cdot C_{qb} \cdot i_g^2 \cdot (V_g - V_{0b})^{x_j} \tag{18}$$

where the constant x_j includes instrumental factors and atomic factors related to spectroscopic and diffusion properties. C_{qb} and V_{0b} are material-dependent constants that determine the sputtering rate in sample segment b; i_g is the current; V_g is the voltage; k_j is a constant characteristic of spectral line j, and c_{ib} is the concentration of element i.

While Bengtson did not use the term "emission yield" in this work, he used the data from the studies of argon lines to derive a related quantity he called an "excitation function". While the current was found to affect the excitation of argon and sample atoms in essentially the same way (a linear increase), Bengtson noted a great difference in the influence of voltage. The possibility of "slight pressure dependence due to the influence of the pressure on the diffusion process" was discussed, but the experimental equipment available did not allow such investigations.

For all of the lines investigated in the first paper, it was found that the intensity increases approximately as the square of the current, and this was therefore assumed to be generally true for all analytical lines. Several examples of experimental data that support this assumption were given. In later work Bengtson et al. [34] found that the square current dependence does not hold true for several emission lines, particularly in the VUV spectral region. Furthermore, the exponential voltage function does not lend itself very well to a quantification algorithm, since it approaches a singularity at the threshold voltage U_{0b}. The empirical intensity expression was therefore modified to the following form:

$$I_{ijb} = k_{ij}\ c_{ib} C_{qb} i_g^{A(j)} f_j(V_g) \tag{19}$$

where the dependence of the EY on the discharge voltage $f_j(V_g)$ is modeled as a polynomial Taylor series developed around the average voltage.

Rf quantification and the pressure dependence of the emission yield

In the previous section we discussed the development of quantification procedures for dc glow discharges. They are based on the measurement of voltage and current. Different approaches were developed to either correct for modifications in the emission yield with varying voltage and/or current or just to maintain fixed electrical parameters by varying the pressure. At the time it was generally considered that although rf-GDOES was interesting and necessary for nonconductive materials, it could not be used for quantitative analysis.

In 1993 R. Payling et al.[35] published a paper showing that both quantitative bulk and surface analysis was possible with rf-GDOES. In this paper Payling compared calibration curves obtained in the rf and dc excitation modes. He found that relative sensitivity factors, using iron as reference, and BEC values for most elements in low alloy steel were the same for dc and rf excitation, at least within a 95% uncertainty interval. He applied these sensitivity factors to the quantification of depth profiles obtained on galvanized steel sheets using both the dc and rf mode. Despite a significant difference between the intensity–time profiles obtained with the two excitation modes, the results, once quantified, were very similar. In the same volume of SIA [36], Payling and Jones showed that the dependence of the emission yield on voltage and current, which was observed in earlier work by Bengtson et al.[34, 37], could be expressed in terms of pressure variation only. Combining the functional dependence of the emission yield on voltage and current and the current–voltage characteristics of the discharge, they found that the emission yield is independent of power but depends strongly on the pressure. Its apparent dependence on voltage and current is only due to the interdependence of the three parameters; current, voltage and pressure. The observation that the emission yield is to a large extent independent of power was later confirmed by Vegiotti [38]. In 1995, Payling et al. [39] compared calibration curves for

different elements (Mn 403 nm, Cu 327 nm) in steel and ZnAl alloy, obtained with different approaches to the emission yield, and based on experiments performed with a dc-GD source. They found that all approaches lead to the same quality of calibration curve, as long as variations in the sputtering rate were taken into account. It was later shown that this approach is not generally applicable, but it presented an important step towards quantifying rf-GDOES depth profiles. Using nonconducting samples, it is not easy to measure the plasma voltage and current. Getting rid of the V,I dependence of the emission yield was therefore the dream of those performing rf measurements!

At the same time Jones et al.[40] published a report on the successful quantification of pigmented polymer coating on steel sheet using rf-GDOES. In this work the authors used a set of painted samples with known stoichiometric compositions, as well as conductive CRMs. The quantification procedure can be considered to be matrix-matched, and the spectral lines are calibrated using similar material to the analyte itself.

In 1995 Payling [41] repudiated the idea that emission yields depend on the pressure only and published work on a new approach. In this work, performed using a dc-GD source, he tested the hypothesis that the emission yield depends on all three external plasma parameters. He assumed the same voltage and current dependencies as suggested earlier by Bengtson. Based on arguments that the influence of the pressure on the emission yield should be linked to the collision probability, he assumed an exponential dependence on pressure. The functional dependence he suggested is given by Eq. 20:

$$R = k \cdot (i_g - i_0)^a \left(V_g - V_0\right)^b P_g \exp\left(-c \cdot P_g\right) \tag{20}$$

where R is the emission yield, i_g is the discharge current, i_0 is an offset current (typically zero), V_g is the discharge voltage, V_0 is an offset voltage (typically 300 V), and P_g is the discharge gas pressure. *a, b* and *c* are regression parameters.

Using a large set of data derived from measurements at different current, voltage and pressure conditions, he determined the best fit values for the parameters *a, b* and *c*.

Figure 1a shows how the current–voltage characteristic of the glow discharge cell significantly depends on the material chosen for use as the cathode. Figure 1b shows the effect of varying the pressure on the emission yield, following the model of Payling. For the majority of elements, or rather spectral lines, (Al 396 nm, Si 288 nm, Cu 327 nm), the variation in the emission yield is within a factor of 2 when the pressure is varied by a factor of little less then 2.5; for Mn 403 nm the variation is less, for Fe 372 nm larger. Increasing the current by a factor of 5 leads to a similar increase in emission yield, and the variation of the emission yield with current is almost linear. Increasing the voltage by a factor of 2 decreases the emission yield by a factor of 2, although most of the changes happen at low voltage, between 400 and 500 V. Due to the offset voltage of 300 V, the variation is far from linear. These results were

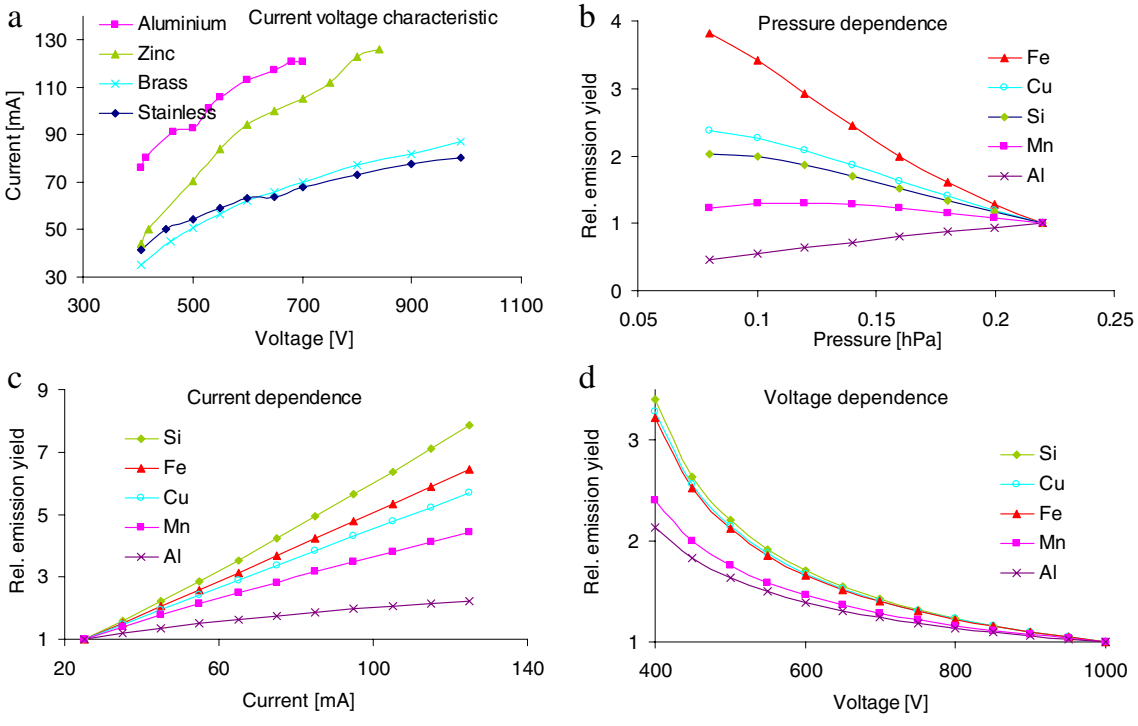

Fig. 1a–d Current–voltage characteristic of dc-GDOES, 7mm anode tube (**a**). Dependence of relative emission yield on discharge gas pressure; the indicated pressure is measured outside the plasma volume; it is lower then the actual gas pressure in the plasma (**b**). Dependence of emission yield on discharge current (**c**). Dependence of emission yield on voltage (**d**). Spectral lines used for the experiment : Al 396 nm, Si 288 nm, Cu 327 nm, Fe 372 nm, Mn 403 nm. Data from Payling [41]

later confirmed by Bengtson using a 4 mm anode tube. Employing an rf source, Bengtson and Hänström [42] found that the rf source did not behave significantly different to the dc source. Summarizing the results obtained in the different series of experiments, we find that the discharge power has little effect on the emission yield. Varying any of the excitation voltage, the discharge current and the pressure has a significant impact on the emission yield. The large spread in the best fit parameters found for different spectral lines and experiments, however, also indicates that the results found so far may have been influenced by details of the experimental set-up, such as the materials used. In particular, the fit parameters obtained for the resonant Al 396 nm, Fe 372nm and Cu 327 nm lines are most likely influenced by the effect of radiation trapping. All three lines are resonant and certainly subject to severe self-absorption in at least one of the materials used.

It is certainly important to understand that all parameters have a significant influence on the emission yield. The important consideration is, however, the impact of these effects on calibration and quantitative analysis, because this is what GDOES is used for. It is therefore interesting to look at the variations in the different parameters when different materials are analyzed.

To graphically illustrate the impact of the variation in the EY with the discharge parameters, an example is given for the effect of emission yield changes in all possible operating modes as you switch from steel to an aluminum sample. Using a steel cathode, the discharge was run at 800 V, 60 mA (48 W) and a resulting pressure of 15.3 hPa. It is impossible to analyze an aluminum sample using exactly the same conditions, because the secondary electron emission yield of aluminum is different to the one of steel. Either the pressure, voltage and/or power must be varied. The resulting operating conditions for an Al sample are summarized in Table 2.

Based on the measured discharge conditions in Table 2, the relative change in EY from the steel reference condition was calculated for the three lines Si 288 nm, Mn 403 nm and Cu 327 nm, see Fig. 1. Equation 20 was used and the constants for the spectral lines from the work of Payling [16]. As an interesting comparison with the work of Payling, the relative emission yield changes due to the electrical parameters in the model according to Bengtson [33] (Eq. 19) are also given. Here, the IU mode shows no relative change since the pressure is ignored as a parameter and is assumed to have zero influence.

As mentioned above, the figure shows that the relative influence of changing pressure in the constant current–constant voltage mode is considerably less than that of changing electrical parameters in all constant pressure modes. These results are confirmed by Marshall's [43] work on multimatrix calibration using different plasma excitation modes, showing that the constant current–constant voltage mode gives calibration curves with a superior fit compared with the constant pressure–constant power mode. Another interesting observation from Fig. 2 is that the experimentally determined influence of the electrical parameters is very similar in the two models, in spite of the fact that Bengtson ignored pressure effects. It should be noted here that the steel–Al couple is close to a worst-case scenario in this respect, as can be seen in Fig. 4.

These results may seem surprising in view of the experimental evidence indicating that over the full operating pressure range, the resulting emission yield can vary by a factor of about 2. An explanation is given the following example. When we combine many different matrices in a single calibration (or a multilayer depth profile) at constant current–voltage, the resulting pressure variations fall in a relatively limited range, producing relatively minor emission yield variations. For the excitation conditions chosen in Table 2, the discharge current increases from 60 mA to 107 mA in the VP mode, whereas the pressure only decreases from 15.3 hPa to 11.1 hPa.

Summarizing, we should state that pressure variations observed during depth profile analysis of different conducting coatings have only a small effect on the emission yield. This, however, does not imply that the pressure can be randomly changed without any influence on the emission yield.

It should also be pointed out that the exact functional dependence of the emission yield on the discharge parameters depends on the data set used to perform the experiment. In particular, studying the influence of pressure requires the use of cathode materials with significantly different secondary electron emission yields. However, it is often then difficult to find samples with known chemical compositions for a large number of elements, common to all samples used for the experiment. The resulting best fit parameters should therefore be interpreted with some care.

Correcting for emission yield changes

Once the dependence of the emission yield on the excitation parameters has been described, it is possible to develop different schemes to correct for the effects of varying the excitation conditions.

The first approach, suggested by Bengtson, is based on measuring the variation in the light intensity with voltage and current. These measured intensities are then fitted to some suitable function, Eq. 18. During the calibration step

Table 2 Glow discharge operating in steel and aluminum

Plasma conditions	Volt	mA	Watt	hPa
Steel	800	60	48	15.3
Al pressure—power (PP)	600	80	48	15.3
Al pressure—current (PI)	450	60	27	15.3
Al pressure—voltage (PU)	800	107	85.4	15.3
Al current—voltage (UI)	800	60	48	11.1

Values in bold characters are kept constant when changing from steel to aluminum

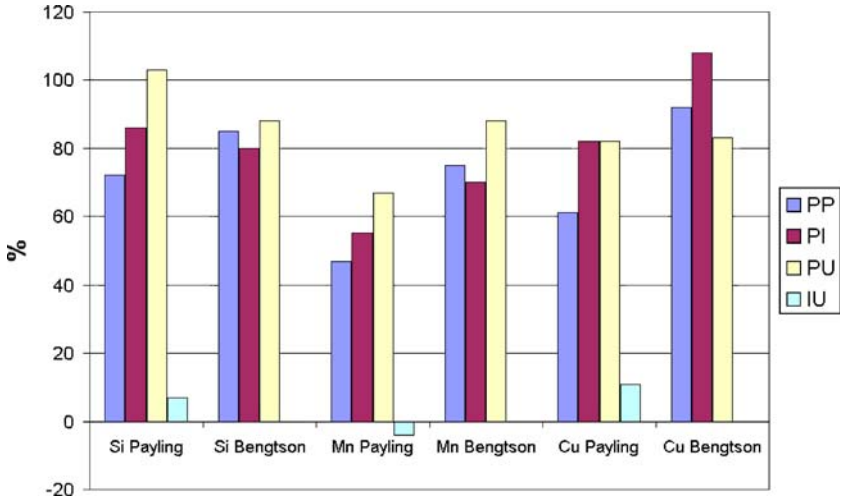

Fig. 2 Relative change in the emission yield between steel and aluminum in the different modes, data from Payling and Jones [62] and Bengtson [63]

voltage and current are kept constant. Given the dependence of the light intensity on the excitation parameters, the effect of variations in these parameters can then be corrected for during the analysis step. The dependence of the emission yield on the pressure is not explicitly taken into account in this approach.

Hocquaux introduced a modification to this approach. He suggested dynamically adapting the pressure, keeping the voltage and current constant independent of the material analyzed. The pressure regulation can be performed during both analyses and calibration. Voltage and current corrections to the emission yield are therefore not necessary. A possible dependence of the emission yield on the pressure is neglected in this approach, as in the earlier approach suggested by Bengtson.

Payling et al. [44–46] suggested operating the source at constant power and pressure and determining the dependence of the emission yield on the voltage and current from the calibration function. This can be achieved by introducing a voltage dependence into the emission yield R_i.

$$c_i q_M = k_i \cdot R_i \cdot I_i - b_i \tag{21}$$

$$R_i = 1 + r_i \cdot \left(V_g - \overline{V}\right) \tag{22}$$

where c_i is the elemental concentration, q_M is the erosion rate, k_i is an instrumental factor, R_i is proportional to the inverse emission yield, I_i is the line intensity, and b_i, the background equivalent concentration, while V_g is the discharge voltage, $\overline{V}$ is an average voltage and r_i is a regression parameter.

Payling introduced this correction as the V_{dc} correction for rf-GDOES, but it can be used for dc-GDOES in just the same way. Operating at constant power and pressure, the dependence of the emission yield on voltage and current can be treated as one parameter, because they are interdependent. The V_{dc} correction to the emission yield in the calibration function accounts for the plasma impedance variations caused by changes in the secondary electron emission yield of the cathode material. Despite its name, it is actually an impedance correction. In this approach, the correction of the emission yield for varying pressure is not required.

Emission yields of the spectral lines of argon

In his early work Bengtson [63] suggested using the ratios of the intensities of analyte lines to the intensities of argon lines. This should make it possible to minimize the effects of varying excitation yields due to variations in the the parameters of the plasma. Looking at the excitation mechanisms, this idea appears very attractive and worthwhile. The excited states of most Ar transitions observed in the visible and UV spectral region are populated through electron impact excitation [47]. Similar processes are responsible for the excitation of most analyte lines of analytical interest. Expressing the analyte spectral line intensity relative to Ar spectral line intensities should therefore attenuate the effect of variations in the excitation probabilities. Experimental results, studying the emission yields of Ar lines as a function of current and voltage, however, show a completely different situation.

When looking at the dependence of the argon intensity on voltage and current for different materials such as iron, brass and aluminum, no significant dependence of the argon intensity can be observed. The measured argon intensities can be fitted to a function of current and voltage:

$$I_{Ar} = k \cdot i_g^{1.46} \cdot f(V_g) \tag{23}$$

where I_{Ar} is the Ar line intensity, k is a constant, i_g is the discharge current and V_g is the discharge voltage. The functional dependence of the emission intensity on the voltage $f(V_g)$ is expressed as a second-order polynomial.

When measuring the emission intensity of the argon line studied (415.8586 nm originating from the {3p5(2P °1.5) 5p2[1.5]2} excited atomic Ar state [48]) using different cathode materials, it was found that the Ar emission increases with both voltage and current. Figure 3a displays the residual errors of a regression calculation that uses Eq. 23 to get the experimentally determined emission inten-

sities as a function of pressure, or rather the gas flow in the discharge cell. Within the range of the experimental data, the flow is approximately proportional to the pressure. The data set includes material leading to different plasma impedances. Obtaining a given voltage and current pair therefore requires different discharge gas pressures. Figure 3a should make any dependence of the argon emission intensity on pressure evident. No such dependence is apparent.

The absolute deviation increases with pressure for Al, and decreases for brass. Although brass and iron show very similar current–voltage characteristics, they show significant differences in terms of the argon emission yield. However, if one looks at the relative intensities I_{obs}/I_{calc}, there is more of a constant matrix-dependent deviation from the average.

In a different experiment performed with an rf glow discharge source, the argon emission intensity of the 404.442 nm line (originating from the same {3p5(2P°1.5) 5p2[1.5]2} [48] excited state of atomic argon) was studied for a large variety of pure materials in order to demonstrate the influence of the secondary electron emission yield, the gas pressure and consequently the source impedance on the argon emission intensity. The experiment was performed in both the constant power and pressure mode as well as the constant voltage and current mode. The materials used and their secondary electron emission yield, γ, are summarised in Table 3. Figure 4 displays the dependence of the source parameters on the secondary electron emission yield, the

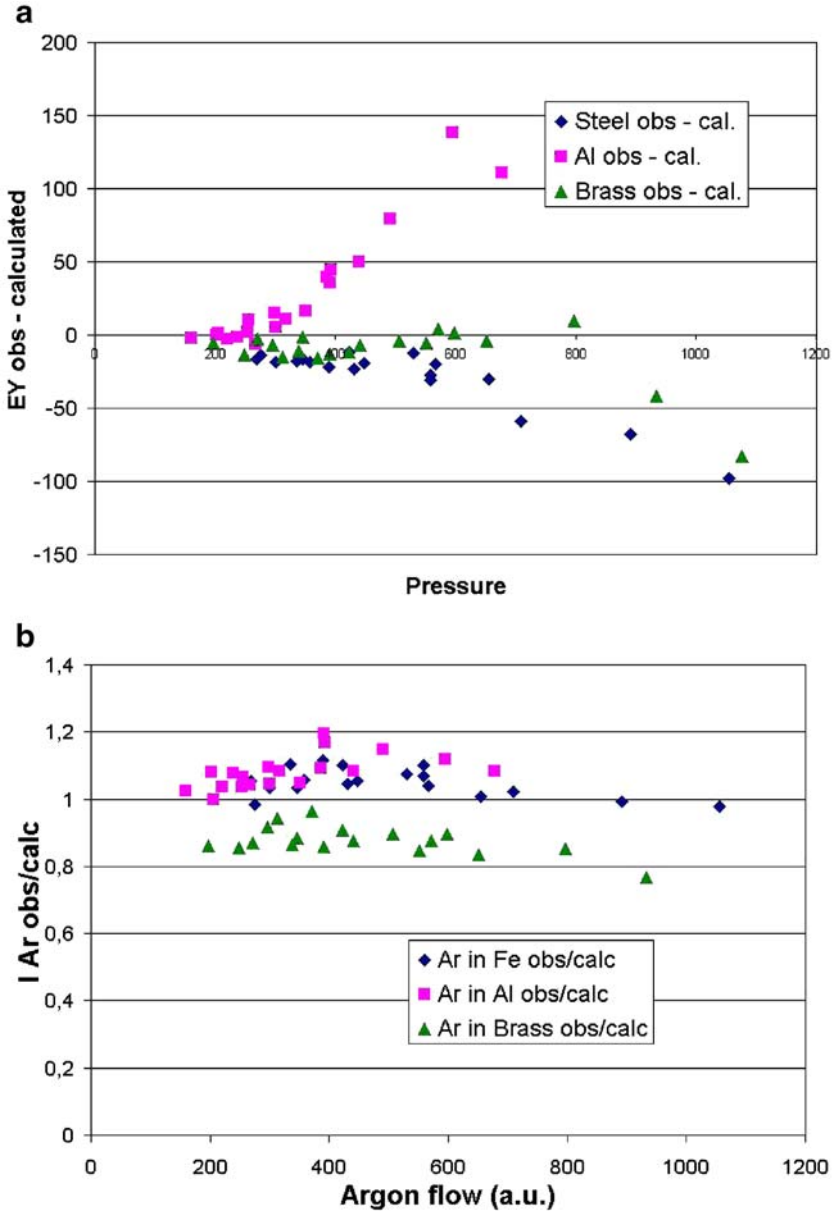

Fig. 3a,b **a** Residual errors from a regression calculation of Ar 415 nm intensities as function of argon flow in different matrices. **b** Observed divided by calculated intensities of Ar 416 nm in different matrices

pressure in the (UI) mode and the voltage in the (PP) mode. γ can be estimated using Eq. 24 [49].

$$\gamma \approx 0.032(0.78\varepsilon_i - 2\Phi_m) \quad (24)$$

where ε_i is the potential energy of the bombarding Ar ion (ε_i=15.8 eV) and Φ_m is the work function of the sputtered solid.

With increasing γ, the dc bias voltage decreases when the pressure is maintained constant (PP mode), and so the pressure needs to be decreased in order to maintain a constant dc bias voltage (UI mode) when γ is increased. The spread of the data is likely to be caused by variations in γ with mechanical and microchemical surface properties, making such estimates rather inexact. Voltage and pressure are clearly correlated in all cases. The estimated values for γ appear to be incorrect in the case of Si, Ag and Pb.

Figure 5 displays the variation of the argon emission for the 404.4 nm spectral line. The measurements performed using Zr as the cathode material are not displayed here, as the this Ar line encounters strong interference with an atomic zirconium line. The results clearly demonstrate that the argon emission is strongly dependent on γ when the pressure is maintained constant and changes in the source impedance are allowed. On the other hand, when the source impedance is maintained constant by varying the pressure, no significant changes are detectable. Therefore, no dependence of the argon emission on the Ar gas pressure is observed, in agreement with the results of Bengtson.

Upon comparing the variation of the argon intensity with the excitation voltage to the variation of the silicon line, it is clear that they exhibit very different behaviors (see Fig. 6).

The argon intensity increases with increasing excitation voltage, while the silicon emission yield decreases. The emission yields of these spectral lines of Si and Ar behave in different ways as the excitation parameters are varied. Normalizing the analyte intensity to argon does not therefore reduce the dependence on the excitation parameters, at least not for the spectral lines studied.

The observation that the light emitted by the argon is independent of the gas pressure does not contradict the observation that the argon emission increases with pressure at constant power, if the cathode material is not changed. In this case the increase in pressure will lead to a decrease in the source impedance. The effect of the rising current on the argon emission intensity is stronger then the effect of decreasing voltage.

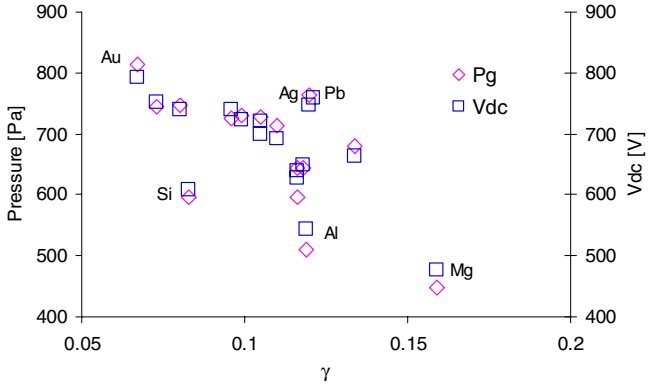

Fig. 4 Dependence of source parameters on sec. elec. em. yield γ for a variety of pure materials; *Pg* represents the carrier gas pressure and *Vdc* is the dc bias voltage. The experimental data were obtained using an rf power of 40 W and a fixed Vdc of 690 V or a fixed argon pressure of 700 Pa, respectively

Inter-element corrections

A general feature of optical emission spectroscopy (OES) is the existence of line overlaps: spectral lines from other elements than the analyte that are sufficiently close to the wavelength of the analyte line to contribute to the signal intensity. Another commonly used term for this effect is line interference. In a sense, line interference is just one part of the signal background, but it must be handled separately in the software since the magnitude of the line interference obviously depends on the content of the interfering element in the sample. Furthermore, line interference is also dependent on the type of light source, since different excitation mechanisms and temperatures strongly influence the relative intensities of the spectral lines.

Table 3 Secondary electron emission yield γ for different pure materials [65]

Element	γ	Vdc [V]	Element	γ	Vdc [V]
Pt	0.054		Sn	0.11	692
Au	0.067	792	Ti	0.116	628
Co	0.073	752	Zn	0.116	640
Ni	0.08	740	V	0.118	648
Si	0.083	608	Al	0.119	544
C	0.086		Ag	0.12	748
Cu	0.096	740	Pb	0.121	760
Mo	0.099	724	Zr	0.134	664
Cr	0.105	700	Mn	0.15	
Fe	0.105	720	Mg	0.159	476

The dc bias voltages were measured using a JY 5,000 RF employing 40 W, 700 Pa and a 4 mm anode

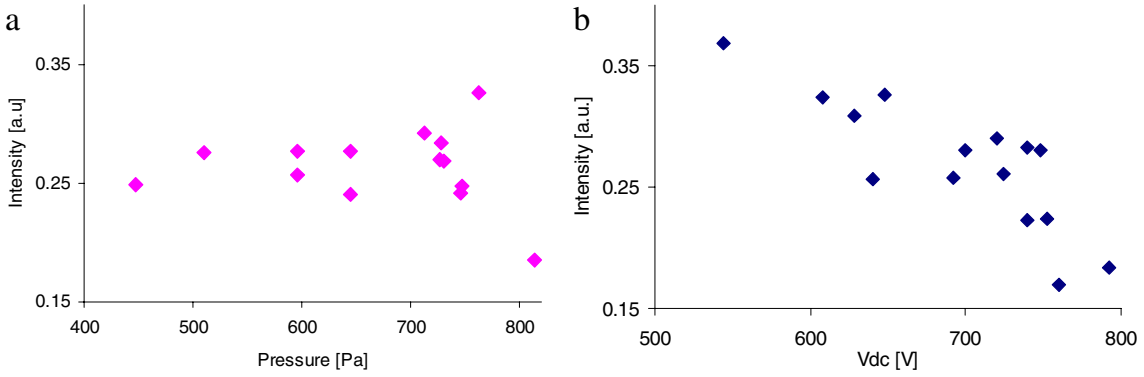

Fig. 5a,b Emission intensity of the argon 404.442 nm line as the secondary electron emission yield is varied; for constant impedance (**a**); for constant pressure (**b**)

Line interference is also highly dependent on the spectrometer optics, since it is affected by the spectral resolution and also the degree of second-order reflection from the grating at the wavelength in question. Also, another reason for line interference can be so-called "ghost" lines in the observed spectrum. These "ghost lines" are caused by periodic imperfections in the grating itself; for example, if every third groove is deeper than the average. These defects are commonly observed on mechanically ruled gratings [50].

Normally, inter-element corrections (IECs) are determined in the regression calculation as part of the calibration function. Provided that there are a sufficient number of calibration samples with a range of concentrations of the interfering element, a least square fit can determine the IEC with statistical certainty. However, this type of calculation must be used with caution. For each IEC, one additional fitting parameter is introduced into the calibration function. It is easy to take this too far, and obtain a perfect fit based on too few calibration samples, using an excessive number of fitting parameters. An alternative method is to determine the IEC by separate measurements on, say, binary standards, and then to enter the IEC constant manually into the calibration function.

Line interferences are important for the analyst using the glow discharge; in particular, the importance of molecular bands is poorly known and often underestimated. In terms of emission yield they are of less importance, as they can be avoided by choosing the material to work with appropriately. More detailed discussion of the subject can be found in the literature [51, 52].

The hydrogen effect

In recent years, it has been discovered that another type of IEC effect, linked primarily to the element hydrogen, can actually affect the EYs and therefore the quantification to a significant extent [54, 55]. It has been shown that the EYs of spectral lines from other elements can be dramatically affected even by very minute concentrations (a few 100 ppm) of hydrogen in the plasma. The hydrogen can originate from the sample itself, contamination due to adsorbed water and pumping oil inside the source, or small vacuum leaks. Both enhancement and suppression effects can be observed for a particular element, depending on the emission line used, showing that the excitation probabilities of excited levels are affected, and it is not "plasma

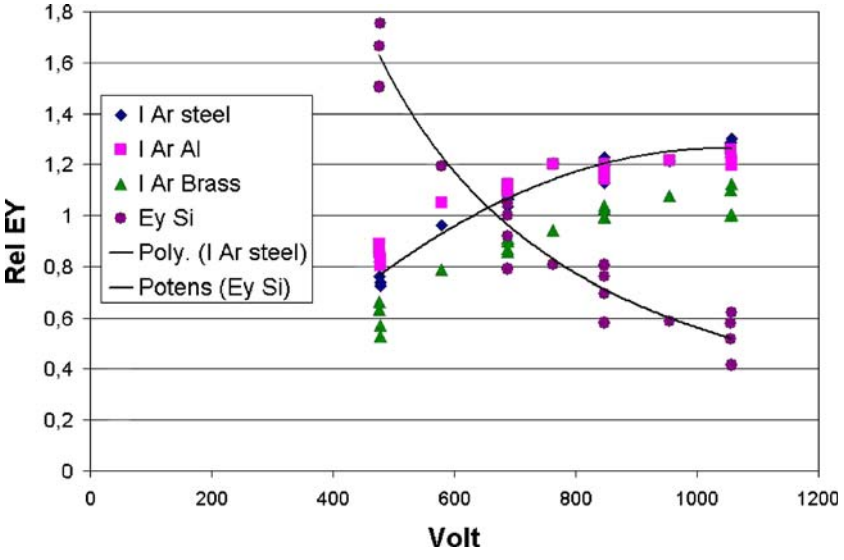

Fig. 6 Difference between the "excitation function" for Ar 415.8 nm and the emission yield of a typical analyte line, here Si 288.2 nm

chemical" reactions at work [54]. In general terms, these effects can be described as a change in the plasma excitation temperature, but the actual mechanisms responsible for this effect are complex [56].

While source contamination and leaks should be minimized by improved source design, the large number of applications where hydrogen is found in the sample itself have made it necessary to introduce matrix correction algorithms to compensate for the EY changes. In fact, this is a true "matrix effect" that violates the earlier assumption that the EYs are matrix-independent. Fortunately, it appears that hydrogen is the element that causes by far the strongest matrix effects of this kind. The effects of different elements such as oxygen and nitrogen have also been studied [53].

At present, there are two practical methods that are used to compensate for the hydrogen effect, both based on the signal intensity from a hydrogen spectral channel. The first method uses a "multiplicative correction" and is therefore unique to each calibration (analytical method). The second method uses an exponential function, where the constants of the exponents are fixed and characteristic of each spectral line. Both methods have their merits and drawbacks, but they have recently been introduced into commercial software from all major manufacturers of GD-OES instruments.

Sputter factors

In 1994 Weiss suggested an interesting approach to multimatrix calibration for GD-OES entirely based on the "constant emission" yield concept. Including line interference, the calibration function for GDOES can be expressed as

$$I_i = R_i q_M c_i + \sum_j a_{ij} I_j + b_i \tag{25}$$

$$q_M = \frac{I_i - \left(\sum_j a_{ij} I_j + b_i \right)}{R_i c_i} \tag{26}$$

where the emission yield R_i is considered to depend only on the specific spectral line used for the element i and is independent of the sample M. In the original calibration procedure suggested by Bengtson, the experimentally derived sputtering rates for all reference material included in the calibration procedure had to be known prior to performing the calibration. Given the large number of calibration samples required for a multimatrix calibration, this requirement is not easily satisfied. To allow calibration samples to be included in the calibration procedures even when the sputtering rate is unknown, Weiss suggested the following procedure.

The calibration procedure is first performed for a restricted set of calibration samples with known sputtering rates. Once the regression parameters for this set are known, the sputtering rate factors q_M are calculated for additional calibration samples based on the calibration curves of a selection of well-suited spectral lines using Eq. 26. These spectral lines must be from elements present in significant concentrations in both the original sample set and the additional samples. The calculation will adjust the sputter factors q_M of the new samples so as to obtain a best fit of the calibration points to the calibration curves of the original set of samples. Using these sputter factors, the new calibration samples can then be included in the enlarged set of calibration samples; this also applies to other elements. This procedure has therefore become a very valuable tool for CDP calibration, particularly when using calibration samples where a direct determination of the sputter factors is technically challenging.

The experimental results showed that the sputter factors derived from such a procedure depend to some extent on the emission lines used and care must therefore be taken when a multimatrix calibration is elaborated based on this approach. The reasons for the observed discrepancies between fitted and measured sputter factors are not yet clearly established. The reflectivity of the calibration samples, the small pressure dependence of the emission yield or other real matrix effects influencing the emission yield may be the source of these discrepancies. In a later publication, Weiss derived a method for estimating the measurement uncertainties in the best-fit parameters.

This iterative calibration procedure can be simplified by linking the analytical functions of all elements together, constructing one large linear regression matrix.

$$q_M c_i = a_i I_i + \sum_j a_{i,j} I_j + b_i \tag{27}$$

For calibration samples with known sputtering rates q_M, the sputtering rate-corrected concentration $q_M c_i$ is treated as aconstant in the regression procedure; if q_M is unknown it will be treated as a variable regression parameter. Linking all of the analytical functions to one large regression matrix in this way requires very good data and a weighted regression procedure that uses realistic estimates of the combined uncertainties of the measurements in order to achieve reasonable results.

Discussion and interpretation

Bogaerts et al. have published several papers on modeling the glow discharge under conditions typically used for mass spectrometry (pressure below 100 Pa) and for the higher pressures used in the Grimm type source. The results of these calculations and models have greatly enhanced our understanding of the properties of the GD source, resulting in greater insight into the major processes that occur in the glow discharge for the analytical glow

discharge community. Bogaerts et al. [54–56] compared experimentally observed line intensities and their dependence on the excitation voltage to results from the model used in their calculation. Although the model reproduced the general trends, a detailed understanding of the observed dependence of the emission yield on plasma parameters has not yet been achieved.

Current dependence

The emission yield increases with the discharge current. For many analyte atomic lines the increase is almost linear. The exponent *a* in Eq. 19, describing the dependence of the EY on current, falls in the range 0.2–1.3 [34], the majority being close to unity. For Ar atoms, the corresponding exponent in Eq. 23 tends to be slightly higher, but there are also considerable variations between spectral lines for Ar. In a GD source, an increase in discharge current can be achieved by various means, either by increasing the power or by decreasing the plasma impedance (i.e., increasing the secondary electron emission yield or the pressure).

The increase in the emission yield, for both Ar and analyte atoms, with the plasma current can be understood, at least to a first approximation. The plasma current is directly linked to the charged particle density in the plasma (Eq. 4). If nothing else is changed in the plasma, increasing the electron density will lead to more efficient excitation of the analyte atoms, in other words increased emission yield (Fig. 1). In a simplistic model one would therefore expect the emission yield to increase linearly with the electron density, hence the plasma current. The fact that significant deviation from the linear dependence is observed for several analytical lines clearly confirms that the processes are more complex. The assumption "if nothing else is changed" does clearly not represent the actual physical reality in the plasma. One obvious effect not taken into account in the simplistic model is the effect of increasing the gas temperature and current. When increasing the current at constant voltage, more power is dumped in the plasma volume. One of the consequences of this is an increase in gas temperature [57]. At constant pressure the increased gas temperature leads to a reduced particle density in the plasma volume. It is still not clear whether an increase of the plasma current at constant power will change the gas temperature or not. Apart from the average variation of the gas temperature, the ion speed in the CDS can be changed if the increase in discharge current has been achieved by increasing the electrical field (Eq. 4). If the current increase has been achieved by varying the secondary electron emission yield, the ratio of electron to ion current will change. In both cases the relationship between discharge current and plasma density will be altered.

Voltage dependence

The effect of the discharge voltage on the light emission is different for analyte atoms and argon atoms. While the light emission of Ar increases with voltage, the emission yield of analyte atoms decreases. The increase in the Ar emission with voltage can be linked to the total energy supplied to the electrons entering the negative glow. Eventually this energy will be lost in collisions and lead to excitation and thermal heating. The exact dependence on the discharge voltage will depend on the detailed excitation mechanism and will therefore be different for lines originating in different excited states.

The significant differences between the analyte emission yields and the argon light emission are most likely linked to the different spatial distributions of these two species in the plasma. The argon atom density is constant, at least approximately, over the entire discharge region; the analyte atom density decreases quickly from its maximum close to the cathode (Fig. 7). The spatial atom distribution maximizes close to the interface between the negative glow and the cathode dark space. The electron density is low in the cathode dark space and has its maximum in the negative glow. The electron distribution in the negative glow is, however, also a function of the energy of the electrons we look at.

The overlap between the electron distribution and the analyte atom distribution is crucial for the emission yield (Eq. 1). It is therefore interesting to look at the evolution of the sheath thickness with discharge voltage.

Following Eq. 7 and Eq. 5, the sheath thickness will increase with increasing discharge voltage, at least if the ion distribution in the CDS is not modified at the time. The

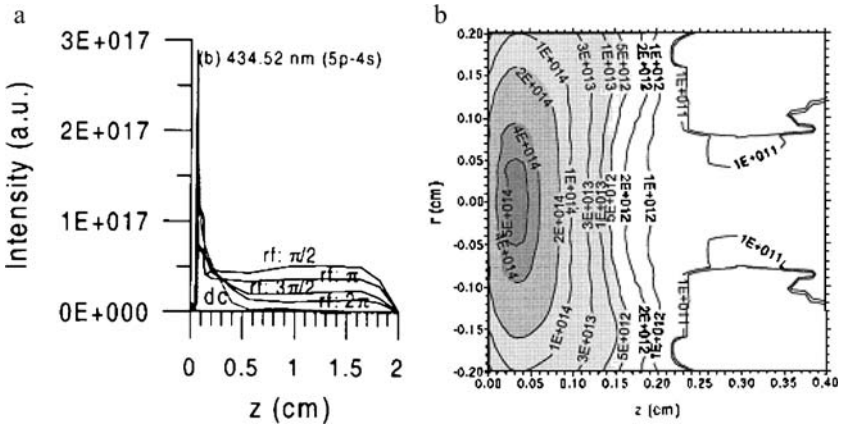

Fig. 7a,b Spatial distribution of atoms in the Grimm source metastable: Ar (**a**) and Cu 0 atoms (**b**); reproduced with the authors' permission from [64]

thermalization process of the neutral atoms sputtered off the cathode surface will not be influenced by the voltage increase. The overlap between the atomic and electronic distributions will decrease and the emission yield should therefore decrease, which is in accordance with the experimental observations. However, the actual processes defining the functional relationship between voltage and emission yield are more complex. For example, Bogaerts et al. report that the length of the CDS decreases slowly with increasing voltage, at least for the low pressures (50–100 Pa) typical of the VG9000 configuration [58]. At the higher pressures maintained in a Grimm-type source, the length of CDS hardly varies with the excitation voltage [10]. In this model the increase in voltage was associated with an increase in current, increasing the ion density and consequently the electrical field. In an empirical model, Aston [59] linked the length of the cathode dark space to the pressure and the plasma current.

An additional effect of discharge voltage on the emission yield is linked to the cross-section for electron excitation (inelastic collision) and its dependence on the electron kinetic energy [A. Bogaerts (CSI, Antwerp, Belgium), 2005, private communication]. The cross-section reaches a maximum for a given electron impact energy. The maximum shifts to a higher value for higher excitation energy. Hence, as the voltage increases the average electron energy increases. For the low-lying excited states typical of many sensitive atomic analyte lines, the maximum has already been passed at normal GD operating parameters, and the cross-section drops. For the higher excitation energies of the Ar lines, it is still on the rise or around the maximum.

Pressure dependence

The carrier gas pressure has a significant influence on the discharge characteristics. When the pressure is increased, the number of collisions per time and volume increases, leading to a drop in the discharge impedance. At constant power the discharge current will therefore increase and the voltage decrease.

The light emitted by the Ar atoms in the plasma does not depend on the gas pressure; or at least such a dependence has not been detected experimentally (Fig. 5). The emission yield of the analyte atoms appears to depend on the pressure, although the exact functional dependence has not yet been clearly established. For most analytical lines studied the emission yield appears to decrease slightly with increasing pressure (Fig. 1b).

When interpreting the effect of pressure on the argon emission, two cases need to be clearly distinguished: operating at constant impedance or constant secondary electron emission yield. When impedance changes are allowed, the variation in current and voltage will induce a change in the light intensity emitted by the argon atoms. When the impedance changes are compensated for by a varying secondary electron emission yield, voltage and current remain constant. As a result the plasma density and the total available energy do not change, so the argon intensity does not change. Minor effects of changing the pressure may be observed due to reduced ion mobility, which changes the relationship between current and ion density in the plasma (Eq. 4). Similarly, the variation of the ratio between electron and ion current in the CDS (Eq. 3) may influence the link between discharge current and charged particle density in the negative glow.

The difference in the emission behavior of analyte atoms and argon upon pressure changes could also be explained by the evolution of the cathode dark space. From experimental data combined with model calculation, presented by Therèse in his thesis, we understand that the cathode dark space will decrease with increasing pressure [60]. Increasing the secondary electron emission yield at constant power and pressure has the opposite effect on the thickness of the CDS [61]. Working at constant impedance, an increase in secondary electron emission yield followed by the decrease in pressure necessary to keep the impedance constant will have only a small effect on the thickness of the cathode dark space. For this reason, the effect of pressure changes on the emission yield is small. The two opposite effects obviously do not compensate entirely, as the emission yield of analyte atoms does show some dependence on the gas pressure.

Conclusions

Quantification procedures for glow discharge optical emission spectroscopy, based on the constant emission yield concept, have become routine work. Although the emission yield can be considered to be nearly independent of the sample material, changes in the secondary electron emission yield influence the source impedance. The impedance change can significantly affect the emission yield. They should, therefore, either be mathematically corrected or the impedance should be kept constant by pressure regulation in order to obtain reliable results from GDOES CDP. The effect ofpressure variation on the emission yield can be considered to be small, within the limits of practical operating conditions for most CDP applications. It should, however, be noted that varying the discharge pressure has a significant effect on the plasma processes and does affect the emission yield when these variations are large. Including the corresponding correction terms in the calibration function might prove sensible if pressure variations are large or the required accuracy is high.

The detailed plasma processes are rather complex. We have tried to extract some basic information in order to better understand the effect of the discharge parameters on the emission yield. A deeper understanding of all processes leading to the enhancement or reduction of emission yield is not possible without detailed simulations and model calculations. Although much progress has been made, a comprehensive description of the effects is not yet available.

Acknowledgements The idea for writing this review article originated during the Richard 'Dick' Payling memorial session at the Winter Plasma Conference at Budapest, Hungary in Jan 2005. Both Arne Bengtson and Thomas Nelis owe a lot of their still limited understanding of the "emission yield" to the numerous discussions with Dick.

The authors thankfully acknowledge the support of Ph. Belenguer, CPAT Toulouse, France, when writing this review article. By patiently answering many of our questions, he has improved the level of our knowledge of basic plasma processes.

References

1. Grove WR (1852) Philos Trans R Soc 142:87
2. Paschen F (1916) Ann Phys 50:901
3. Chapman B (1942) Glow discharge processes. Wiley, New York
4. Marcus RK (1993) Glow discharge spectroscopies. Plenum, New York
5. Markus RK, Broekaert JAC (2003) Glow discharge plasmas in analytical spectroscopy. Wiley, Chichester, UK
6. Bings NH, Bogaerts A, Broekaert JAC (2004) Anal Chem 76:3313–3336
7. Grimm W (1967) Natur Wiss 54:586
8. Nelis Th, Pallosi J (2006) GDOES and MS as tool for surface and interface analysis. Appl Spectrosc Rev (in press)
9. Bogearts A, Gijbels R (1998) Modelling of argon direct current glow discharges and comparison with experiment: how good is the agreement? J Anal Atom Spectrom 13:945–953
10. Bogaerts A, Gijbels R (1998) Comprehensive description of a Grimm-type glow discharge source used for optical emission spectrometry: a mathematical simulation. Spectrochim Acta B 53:437–462
11. Gamez G, Huang M, Lehn SA, Hiiftje GM (2003) Laser-scattering instrument for fundamental studies on a glow discharge. J Anal Atom Spectrom 18:680–684
12. Winchester MR, Payling R (2004) Spectrochim Acta B 59: 607–666
13. Bogaerts A, Gijbels R (1999) Monte Carlo model for the argon ions and fast argon atoms in a radio-frquency discharge. IEEE T Plasma Sci 27(5):1406–1415
14. Belenguer Ph, Guillot Ph, Therese L (2003) Electrical characterization of radiofrequency glow discharge used for optical emission spectroscopy. Surf Interf Anal 35:604–610
15. Nelis Th, Payling R (2004) A guidebook to glow discharge optical emission spectroscopy. RSC, Cambridge
16. Payling R (1997) In: Payling R, Jones DJ, Bengtson A (eds) Glow discharge optical emission spectroscopy. Wiley, Chichester, UK, Chap. 8.6
17. Bogaerts A, Gijbels R, Carman RJ (1998) Collisional-radiative model for the sputtered copper atoms and ions in a direct current argon glow discharge. Spectrochim Acta B 53: 1679–1703
18. Weiss Z (1997) J Anal Atom Spectrom 12:159–164
19. Nelis Th, Aeberhard M, Hohl M, Rohr L, Michler J (2006) Characterisation of a pulsed rf-glow discharge in view of its use in OES. J Anal Atom Spectrom 21:1–14
20. Nobory Y (1994) Rigaku Inc. Japanese patent. No.JP6043100
21. Hoffmann V, Kurt R, Kämmer K, Thielsch R, Wirth Th, Beck U (1999) Interference phenomena at transparent layers in glow discharge optical emission spectrometry. Appl Spectrosc 53 (8):987–990
22. Kimura S, Mitsui Y (2001) Effect of optical interferences on BPSG profiles obtained with a GDOES. Appl Spectrosc 55 (3):292–297
23. Wilken L, Hoffmann V, Wetzig K (2003) J Anal Atom Spectrom 18:1141
24. Berneron R, Charbonier JC (1981) Surface analysis by glow discharge. Surf Interf Anal 3(3):134–141
25. Takadoum J, Pivin JC, Pons-Corbeau J, Berneron R, Charbonier JC (1984) Comparative study of ion implantation profiles in metals. Surf Interf Anal 6(4):174–183
26. Pons-Corbeau J, Cazet JP, Moreau JP, Berneron R, Charbonnier JC (1986) Quantitative surface analysis by glow discharge optical spectrometry. Surf Interf Anal 9:21–25
27. Pons-Corbeau J (1985) Study of emission and sputtering yields in some alloys and oxide by glow discharge optical spectrometry: quantification of analysis. Surf Interf Anal 7(4):160–176
28. Nelis T, Aeberhard M, Payling R, Michler J, Chapon P (2004) J Anal Atom Spectrom 19:1354–1360
29. Suzuki K, Nishizaka K, Ohtsubo T (1984) T Iron Steel Inst Jpn 24:B–259
30. Suzuki M, Kojima R, Suzuki K, Nishizaka K, Ohtsubo T (1985) T Iron Steel Inst Jpn 25:B–220
31. Payling R (1997) In: Payling R, Jones DJ, Bengtson A (eds) Glow discharge optical emission spectroscopy. Wiley, Chichester, UK
32. Nelis T, Payling R (2004) Glow discharge optical emission spectroscopy: a practical guide. RSC, Cambridge
33. Bengtson A (1985) Spectrochim Acta Part B 40:631
34. Bengtson A, Eklund A, Lundholm M, Saric A (1990) J Anal Atom Spectrom 5:563
35. Payling R, Jones DG, Gower SA (1993) Quantitative analysis with dc and rf glow discharge spectrometry. Surf Interf Anal 20:939–966
36. Payling R, Jones DG (1993) Fundamental parameters in quantitative depth profiling and bulk analysis with glow discharge spectrometry. Surf Interf Anal 20:787–793
37. Bengtson A, Danielsson L (1985) Thin Solid Films 123:231
38. Vegiotti JP (1997) Engineering thesis. Conservatoire National des Arts et Metiers, Paris, p 49
39. Payling R, Jones DG, Gower SA (1995) In search of the ultimate experiment for QDP in GDOES part I. Surf Interf Anal 23:1–11
40. Jones DG, Payling R, Gower SA, Boge EM (1993) Analysis of pigmented polymer coatings with rf gdoes. Surf Interf Anal 20:369–373
41. Payling R (1995) In search of the ultimate experiment for quantitative depth profile analysis in glow discharge optical emission spectrometry. Part II: Generalized method. Surf Interf Anal 23:12–21
42. Bengtson A, Hänström S (1998) Emission yield for CDP-parameters. J Anal Atom Spectrom 13:437–441
43. Marshall K (1990) J Anal Atom Spectrom 14:923
44. Payling R, Aeberhard M, Delfoss D (2000) Glow discharge analysis of hard coatings and metallic coatings on steel. In: 12th Int Federation for Heat Treatment and Surface Engineering Congress, 29th Oct–2 Nov 2000, Melbourne, Australia
45. Payling R, Aeberhard M, Delfoss D (2001) Improved quantitative analysis of hard coatings by radiofrequency glow discharge optical emissio spectrometry (rf-GDOES). J Anal Atom Spectrom 16:50–55
46. Payling R, Michler J, Aeberhard M (2002) Quantitative analysis of conductive coatings by radiofrequency powered glow discharge optical emission spectrometry: hydrogen, d.c. bias voltage and density corrections. Surf Interf Anal 33: 372–477
47. Bogaerts A, Gijbels R (2000) Ar spectrum. Spectrochim Acta Part B 55:263–278
48. Larkins P, Payling R (2000) Optical emission lines of the elements. Wiley, Chichester, UK
49. Therèse L (2005) Thesis. Univ. Toulouse III, France, p 81
50. Nelis Th (1997) In: Payling R, Jones DJ, Bengtson A (eds) glow discharge optical emission spectroscopy. Wiley, Chichester, UK
51. Payling R, Brown NV, Gower SA (1994) Correcting for background and inter element effects in glow discharge optical emission spectrometry. J Anal Atom Spectrom 9:363
52. Bengtson A (2003) CDP organic coating—molecular bands. J Anal Atom Spectrom 18:1066–1068

53. Fernandez B, Bordel N, Pereiroa R, Sanz-Medel A (2003) Investigations of the effect of hydrogen, nitrogen or oxygen on the in-depth profile analysis by radiofrequency argon glow discharge-optical emission spectrometry. J Anal Atom Spectrom 18:151–156
54. Boegaerts A, Guernard RD, Smith BW, Wineforder JD, Harrison WW, Gijbels R (1997) Three-dimensional density profiles of argon metastable atoms in a direct current glow discharge: experimental study and comparison with calculations. Spectrochim Acta B 53:219–229
55. Bogaerts A, Gijbels R, Vlcek J (1998) Modeling of glow discharge optical emission spectrometry: calculation of the argon atomic optical emission spectrum. Spectrochim Acta B 53:1517–1526
56. Bogaerts A, Gijbels R (1998) Argon and copper optical emission spectra in a Grimm glow discharge source: mathematical simulations and comparison with experiment. J Anal Atom Spectrom 13:721–726
57. Ferreira NP, Strauss JA, Human HGC (1983) Developments in glow discharge emission spectrometry. Spectrochim Acta 38B:899–911
58. Bogaerts A, Gijbels R (1998) J Anal Atom Spectrom 13: 945–953
59. Aston FW (1907) P Roy Soc Lond A Mat 78:80
60. Therèse L (2005) Thesis. Univ. Toulouse III, France, p 140 (Fig. 5–54)
61. Therèse L (2005) Thesis. Univ. Toulouse III, France, p 149 (Fig. 5–71)
62. Payling R, Jones DJ (1993) Fundamental parameters in quantitative depth profile analysis with glow discharge spectometry. Surf Interf Anal 20:787–793
63. Bengston A (1994) Spectrochim Acta 29B:411
64. Bogaerts A, Gijbels R (2000) Behavior of the sputtered copper atoms, ions and excited species in a radio-frequency and direct current glow discharge. Spectrochim Acta B 55:279–297
65. Therèse L (2005) Thesis. Univ. Toulouse III, France, p 74